

Quantum Geometric Limits for Non-Abelian Holonomies

François Impens¹ and David Guéry-Odelin²

¹*Instituto de Física, Universidade Federal Rio de Janeiro, 21941-972 Rio de Janeiro, RJ, Brazil*

²*Laboratoire Collisions Agrégats Réactivité, UMR 5589, FERMI, Université de Toulouse, CNRS, 118 Route de Narbonne, 31062 Toulouse CEDEX 09, France.*

(Dated: May 28, 2026)

Stokes' theorem turns Abelian Berry phases into curvature fluxes, whereas path ordering precludes such a simple formula for non-Abelian holonomies. We show that a quantitative form of this intuition survives: arbitrary Wilczek–Zee holonomies obey a universal quantum geometric limit (QGL), in which the holonomy magnitude is bounded by a surface integral of the non-Abelian curvature norm. Recasting holonomic evolution as an effective Stokes–Schrödinger dynamics driven by transported curvature, we identify the QGL as the geometric counterpart of conventional quantum speed limits, with a time-integrated generator norm replaced by a surface-integrated curvature cost. The induced contour–surface variational problem is governed by a non-Abelian Lorentz force, which we address with a brachistochrone ansatz of curvature-weighted geodesics. Applied to an $SU(2)$ tripod dark subspace, near-optimal protocols spontaneously align the transported curvature along a single Lie-algebra direction, effectively taming non-Abelianity.

Geometric phases reveal that quantum evolution is not governed solely by dynamical phases, but also by the geometry of the path followed in parameter space [1–4]. In the adiabatic regime, this geometric structure takes the form of parallel transport generated by a gauge connection and its associated curvature [5, 6]. For a nondegenerate state the resulting holonomy reduces to the Abelian Berry phase. In the presence of degeneracies, however, the transported eigenspace is multidimensional, and the adiabatic connection becomes matrix-valued. Closed paths then generate non-Abelian Wilczek–Zee holonomies, which act as unitary transformations within the degenerate subspace and provide the basis of holonomic quantum gates [5, 7–11].

This geometric viewpoint has become increasingly relevant experimentally: non-Abelian geometric phases and holonomic transformations have been explored on a broad range of quantum platforms, including trapped ions [12, 13], cold atoms [14–19], superconducting circuits [20, 21], solid-state spins [22–24] and photonic systems [25–29]. These developments naturally raise the question of the fundamental geometric resources required to implement a prescribed holonomy. The Abelian Berry phase, equal to the curvature flux through any surface bounded by the loop, provides the basic geometric intuition. In the non-Abelian case, however, the situation is fundamentally subtler. Path ordering prevents the logarithm of the holonomy from being written as a simple curvature flux. The central question is therefore whether one can nevertheless derive a universal geometric bound for non-Abelian holonomies, and formulate the corresponding optimization as a variational holonomic control problem.

This is the program of the present work. In ordinary quantum speed limits (QSLs), the distance travelled in Hilbert or unitary space is bounded by the time integral of a dynamical generator norm, typically char-

acterized by the energy uncertainty [30–42]. Recently, isoholonomic QSLs have been derived for cyclic quantum evolutions, bounding the length of one-dimensional trajectories in state or density-operator space [43]. Unlike these QSLs, holonomic transformations generated by Wilczek–Zee connections arise from closed loops in control-parameter space. This motivates the concept of a quantum geometric limit (QGL), in which the dynamical resource of conventional QSLs is replaced by a geometric surface density determined by the non-Abelian curvature and integrated over a spanning surface bounded by the loop. In practice, a minimal time scale would emerge in the presence of constraints on control velocities, spectral gaps, or admissible adiabatic errors.

We begin by deriving a differential form of the non-Abelian Stokes theorem [44–46] adapted to holonomic evolution. By encoding a line integral into the geometric generator, this representation restores an effective one-dimensional evolution equation naturally leading to universal geometric bounds for holonomies. For a prescribed target holonomy U^* , the resulting QGL defines a geometric cost for any spanning surface and turns the search for optimal implementations into a coupled variational problem over contours \mathcal{C} and spanning surfaces $\Sigma(\mathcal{C})$ bounded by \mathcal{C} . Beyond the bound itself, this variational formulation provides a constructive route toward protocols approaching the geometric limit. While the full problem is nonlocal and very challenging, we adapt the time-optimal framework of quantum brachistochrones [47–49] to construct approximate near-optimal solutions in the non-Abelian holonomic setting. The resulting candidate contours satisfy driven geodesic equations in a curvature-weighted metric, with a Lorentz-force term generated by the non-Abelian curvature. We illustrate these principles in the degenerate dark subspace of a four-level tripod atomic system. More broadly, the framework applies to adiabatically controlled systems supporting degener-

ate subspaces, including Λ and tripod configurations encountered in quantum optics and atomic physics [50–53]. *Non-Abelian transport and Fubini–Study metric.* We consider the non-Abelian adiabatic transport of a quantum state $|\psi(\boldsymbol{\lambda}(t))\rangle = \sum_{n=1}^N c_n(\boldsymbol{\lambda}(t))|D_n(\boldsymbol{\lambda}(t))\rangle$ within an N -dimensional degenerate subspace \mathcal{H}_N along a closed path \mathcal{C} in parameter space. This evolution generates a unitary gate

$$U(\mathcal{C}) = \mathcal{P} \exp\left(i \oint_{\mathcal{C}} A_{\mu} d\lambda^{\mu}\right) \quad (1)$$

acting on the initial coefficient vector $\mathbf{c}(\boldsymbol{\lambda}(0))$. $A_{\mu}(\boldsymbol{\lambda})_{ab} = i \langle D_a(\boldsymbol{\lambda}) | \partial_{\mu} D_b(\boldsymbol{\lambda}) \rangle$ is the Wilczek–Zee connection. The path-ordering \mathcal{P} is essential as generally $[A_{\mu}(\boldsymbol{\lambda}), A_{\nu}(\boldsymbol{\lambda}')] \neq 0$, and $U(\mathcal{C})$ depends on the full path \mathcal{C} . The choice of basis $\{|D_n(\boldsymbol{\lambda})\rangle\}$ along the path defines an $SU(N)$ gauge freedom. For closed paths, $U(\mathcal{C})$ transforms only by a single conjugation under local basis changes. Its conjugacy class then encodes gauge-invariant properties of the non-Abelian holonomy, in analogy with the Berry phase. The variation of the degenerate subspace with the control parameters induces a natural Riemannian metric on the parameter manifold \mathcal{M} . Let $P(\boldsymbol{\lambda}) = \sum_{a=1}^N |D_a(\boldsymbol{\lambda})\rangle \langle D_a(\boldsymbol{\lambda})|$ denote the projector onto $\mathcal{H}_N(\boldsymbol{\lambda})$. The Fubini–Study metric on the manifold of degenerate subspaces is then defined as $ds^2 = \frac{1}{2} \text{Tr}(dP dP) = g_{\mu\nu}(\boldsymbol{\lambda}) d\lambda^{\mu} d\lambda^{\nu}$, which is gauge-invariant and measures the distinguishability of nearby subspaces [48]. The metric $g_{\mu\nu}$ provides the geometric structure underlying both the QGL framework developed below and the quantum brachistochrone formulation.

Curvature flux and Berry phase. In the Abelian case, the geometric cost of a closed adiabatic cycle is directly controlled by curvature flux. Indeed, Stokes’ theorem gives $\Phi[\mathcal{C}] = \iint_{\Sigma(\mathcal{C})} F_{\mu\nu}(\boldsymbol{\lambda}) d\Sigma^{\mu\nu}$, for any surface $\Sigma(\mathcal{C})$ bounded by \mathcal{C} . If $|F_{\mu\nu}| \leq F_{\max}$ on the accessible parameter manifold \mathcal{S} , one obtains $\mathcal{A}_{\Sigma} \geq |\Phi[\mathcal{C}]|/F_{\max}$. For a spin- $\frac{1}{2}$ in a slowly varying magnetic field, $H = -\mathbf{B} \cdot \boldsymbol{\sigma}$, with $\mathbf{B} = B(\sin \theta \cos \phi, \sin \theta \sin \phi, \cos \theta)$, the curvature satisfies $|F_{\theta\phi}| \leq 1/2$. Thus a Berry phase $\Phi[\mathcal{C}] = \pi$ requires $\mathcal{A}_{\Sigma} \geq 2\pi$, i.e. at least a hemisphere of the Bloch sphere, and this bound is saturated because $\Phi[\mathcal{C}] = \Omega(\Sigma)/2$. This Abelian example illustrates the emergence of a minimal geometric cost associated with holonomic evolution.

Effective Stokes–Schrödinger dynamics. We construct a non-Abelian Stokes representation [44, 46, 54] specifically adapted for the present geometric setting. More precisely, the holonomy problem can be recast as an effective one-dimensional Schrödinger equation in the Stokes representation [55]

$$\partial_{s_1} V = -i\mathcal{K}(s_1)V \quad (2)$$

where $V(s_1)$ is a unitary evolution operator satisfying $V(0) = \mathbb{I}$ and $V(1) = U(\mathcal{C})$. The strip generator $\mathcal{K}(s_1)$ acts as an effective Hamiltonian and is constructed

from the non-Abelian curvature transported to a common base point on the surface [55]. Explicitly, $\mathcal{K}(s_1) = \int_0^1 ds_2 \tilde{F}_{s_1 s_2}(s_1, s_2)$ in terms of the projected curvature $\tilde{F}_{s_1 s_2}(s_1, s_2) = \tilde{F}_{\mu\nu}(\boldsymbol{\lambda}_{\Sigma}(s_1, s_2)) \partial_{s_1} \lambda_{\Sigma}^{\mu} \partial_{s_2} \lambda_{\Sigma}^{\nu}$. The latter captures the geometry of the parametrized surface $\boldsymbol{\lambda}_{\Sigma}(s_1, s_2)$ through the tangent vectors $\partial_{s_1} \boldsymbol{\lambda}_{\Sigma}$ and $\partial_{s_2} \boldsymbol{\lambda}_{\Sigma}$. Equation (2) yields a natural QSL-like framework, in which the relevant resource is the curvature encoded in $\mathcal{K}(s_1)$ instead of the energy variance associated with a standard Hamiltonian. The resulting QGL originates from the geodesic distance associated with the effective unitary evolution (2), in close analogy with ordinary QSLs, which arise from geodesic distances in the Fubini–Study geometry [31]. Unlike ordinary Hamiltonian dynamics, however, the strip generator $\mathcal{K}(s_1)$ itself is obtained from a line integral – thus leading to QGLs given by surface integrals.

Hilbert–Schmidt QGL for non-Abelian holonomies. Starting from the Stokes–Schrödinger equation (2), one can first transpose the QSL derivation by Vaidman [56], recently extended to unitary gates [41], to the QGL setting. This approach, based on elementary arguments, yields a Mandelstam–Tamm QGL relating the integrated curvature norm to the overlap of the target holonomy with the identity [55]:

$$\arccos \left| \frac{1}{N} \text{Tr} U(\mathcal{C}) \right| \leq \iint_{\Sigma(\mathcal{C})} \|F(\boldsymbol{\lambda})\|_{\text{HS}} dS. \quad (3)$$

Here the overlap reduces to a simple trace. From now on, we use the Hilbert–Schmidt norm $\|A\|_{\text{HS}} = \sqrt{\langle A, A \rangle}$ with inner product $\langle U, V \rangle = \text{Tr}(U^{\dagger} V)/N$. Also, $\|F(\boldsymbol{\lambda})\|_{\text{HS}} = \sqrt{\frac{1}{2} \langle F_{\mu\nu}, F^{\mu\nu} \rangle}$. In the QGLs (3–5), dS is the gauge-invariant area element induced on $\Sigma(\mathcal{C})$ by the Fubini–Study metric (see [55]).

Considering instead the geodesic distance leads to a more fundamental bound for any loop \mathcal{C} and any smooth spanning surface $\Sigma(\mathcal{C})$ (see [55]):

$$\|\log_{\min} U(\mathcal{C})\|_{\text{HS}} \leq \iint_{\Sigma(\mathcal{C})} \|F(\boldsymbol{\lambda})\|_{\text{HS}} dS. \quad (4)$$

$\log_{\min} U$ denotes the minimal logarithm, and $\Theta(U) \equiv \|\log_{\min} U\|_{\text{HS}}$ defines a gauge-invariant measure of gate magnitude, reducing to the usual rotation angle for $SU(2)$. Equation (4) defines an intrinsic QGL and sets a minimal geometric cost for generating a prescribed holonomy. The associated resource is the non-Abelian curvature-norm density integrated over a spanning surface. For a fixed holonomy $U(\mathcal{C})$, the bound (4) holds for any smooth spanning surface $\Sigma(\mathcal{C})$ and can therefore be optimized over the surface choice. More generally, the minimal geometric cost of a target gate U^* is obtained by minimizing the right-hand side over all loops \mathcal{C} satisfying $U(\mathcal{C}) = U^*$ and all spanning surfaces $\Sigma(\mathcal{C})$. This defines a coupled optimization problem over contours and sur-

faces, which admits a variational formulation discussed below.

Operator-norm QGL for non-Abelian holonomies. A tighter universal QGL bound follows from Eq.(2) [55],

$$\|\log_{\min} U(\mathcal{C})\|_{\text{HS}} \leq \iint_{\Sigma(\mathcal{C})} \|F(\boldsymbol{\lambda})\|_{\text{op}} dS. \quad (5)$$

This bound is obtained by viewing the non-Abelian curvature as a map acting on antisymmetric bivectors, $T_F : B^{\mu\nu} \mapsto F_{\mu\nu}(\boldsymbol{\lambda})B^{\mu\nu}/2$. Precisely, $\|F(\boldsymbol{\lambda})\|_{\text{op}}$ denotes the operator norm $\|F\|_{\text{op}} := \sup_{B \neq 0} \|\frac{1}{2}F_{\mu\nu}B^{\mu\nu}\|_{\text{HS}}/\|B\|_{\text{vec}}$, with $\|B\|_{\text{vec}} = \sqrt{\frac{1}{2}B_{\mu\nu}B^{\mu\nu}}$. At the price of involving a less tractable geometric norm, the operator-norm bound (5) is always as tight as, or tighter than, the Hilbert–Schmidt bound (4) [55]. It therefore defines the sharpest QGL for non-Abelian holonomies, while the relaxed Hilbert–Schmidt QGL (4) remains particularly useful for the construction of near-optimal protocols.

Surfaces with effectively Abelian transported curvature. We now consider the special case of spanning surfaces $\Sigma(\mathcal{C})$ for which the transported curvature field remains everywhere collinear with a fixed Lie-algebra generator. The existence of such surfaces depends both on the underlying curvature field and on the chosen contour. In this regime, the strip generators $\mathcal{K}(s_1)$ commute, path ordering drops out from Eq. (2), and the holonomy reduces to an ordinary exponential. For such surfaces, the obstruction associated with non-commutativity is lifted, and the bound reduces to a direct non-Abelian generalization of the Berry-curvature flux relation [55], with the Hilbert–Schmidt norm replacing the absolute value.

Non-Abelianity and QGL saturation. In the Abelian case, saturation of the geometric bound is achieved by choosing a surface whose local orientation is everywhere adapted to the curvature field. For generic non-Abelian holonomies, the situation is more subtle, since variations in the Lie-algebra direction of the transported curvature hinder a globally coherent flux accumulation. Nevertheless, in the examples considered below, near-optimal solutions exhibit an approximate alignment of the transported curvature over the optimized surface $\Sigma(\mathcal{C})$.

Non-Abelian QGL optimization. We formulate the QGL optimization as a variational problem minimizing the Hilbert–Schmidt bound (4) for a target gate U^* . We introduce the action $S[\boldsymbol{\lambda}_\Sigma, \boldsymbol{\lambda}_\mathcal{C}, K_0] = S_{\text{Geo}}[\boldsymbol{\lambda}_\Sigma] + S_{U^*}[K_0, \boldsymbol{\lambda}_\mathcal{C}]$, where $S_{\text{Geo}}[\boldsymbol{\lambda}_\Sigma] = \iint_{\Sigma(\mathcal{C})} \|F\|_{\text{HS}} dS$ measures the geometric cost, and $S_{U^*}[K_0, \boldsymbol{\lambda}_\mathcal{C}]$ enforces the target holonomy. The contour $\boldsymbol{\lambda}_\mathcal{C}$ determines the holonomy, while the surface $\boldsymbol{\lambda}_\Sigma$ controls the geometric cost, leading to a coupled optimization over paths and surfaces. Here $K_0 \in \mathfrak{su}(N)$ is a constant anti-Hermitian Lie-algebra multiplier acting as a geometric generator.

Stationarity with respect to K_0 enforces $U(\mathcal{C}) = U^*$, while variation with respect to the surface and contour yields bulk and boundary conditions (see [55]). We

henceforth parametrize the contour by $t \in [0, T]$, with $s_1 \equiv t/T$. Variation yields the boundary equation for the optimal contour:

$$\|F(\boldsymbol{\lambda}_\mathcal{C}(t))\|_{\text{HS}} \hat{t}_\mu = \text{Re Tr} \left[i K(t) F_{\mu\nu}(\boldsymbol{\lambda}_\mathcal{C}(t)) \dot{\lambda}_\mathcal{C}^\nu(t) \right], \quad (6)$$

where \hat{t}^μ is the outward surface traction vector and $K(t) = U(t)^{-1}K_0U(t)$ is the adjoint-transported generator along the contour. Equation (6) has the form of a non-Abelian Lorentz-force law for the boundary loop: the left-hand side describes an effective surface tension, while the right-hand side corresponds to a gauge-field force induced by the holonomy.

Effective QGL optimization via non-Abelian quantum brachistochrone – The coupled loop–surface equations define a challenging nonlocal problem. As an effective approximation, we use the geometric intuition that shorter boundary loops provide natural candidates for lower spanning-surface costs. To capture, at the contour level, the curvature-norm weighting of the QGL cost, we introduce the conformally rescaled metric $g'_{\mu\nu} = \|F\|_{\text{HS}} g_{\mu\nu}$. We thus solve the corresponding brachistochrone problem under the holonomy constraint $U(T) = U^*$ and a closure constraint, and then minimize the geometric functional $S_{\text{Geo}}[\boldsymbol{\lambda}_\Sigma]$ over all spanning surfaces bounded by the resulting loop. This provides an effective decoupling of the complete loop–surface problem.

To obtain contour candidates, we formulate a non-Abelian brachistochrone problem in the curvature-weighted metric. In the standard brachistochrone formulation, among all paths $\boldsymbol{\lambda}(t)$ implementing the target holonomy U^* , one seeks the path of shortest Fubini–Study length $\mathcal{L} = \int_0^T dt \sqrt{g_{\mu\nu}(\boldsymbol{\lambda}) \dot{\lambda}^\mu \dot{\lambda}^\nu}$. For a fixed time interval, this is equivalent to minimizing the energy functional

$$J_L[\boldsymbol{\lambda}, \dot{\boldsymbol{\lambda}}] = \frac{1}{2} \int_0^T dt g_{\mu\nu}(\boldsymbol{\lambda}) \dot{\lambda}^\mu \dot{\lambda}^\nu, \quad (7)$$

under the constraint $U(T) = U^*$ [57], with the path velocities $\dot{\boldsymbol{\lambda}}$ as controls. The minimizing parametrization has constant Fubini–Study speed, yielding $J_L[\boldsymbol{\lambda}, \dot{\boldsymbol{\lambda}}] = \mathcal{L}^2/(2T)$. For the QGL contour ansatz, the same construction is applied in the curvature-weighted metric $g'_{\mu\nu}$. Applying the Pontryagin maximum principle [58] yields a driven geodesic equation (see [55]),

$$\ddot{\lambda}^\mu + \Gamma_{\alpha\beta}^\mu[g'] \dot{\lambda}^\alpha \dot{\lambda}^\beta = \mathcal{D}_{\text{QGL}}^{\mu\nu(K)}(\boldsymbol{\lambda}, t) \dot{\lambda}_\nu. \quad (8)$$

$\mathcal{D}_{\text{QGL}}^{\mu\nu(K)} = i \langle K(t), F^{\mu\nu} \rangle / \|F\|_{\text{HS}}$ denotes the projection of the normalized curvature onto the transported generator $K(t)$. Since $K(t)$ is anti-Hermitian, the factor i ensures that $\mathcal{D}_{\text{QGL}}^{\mu\nu(K)}$ is real. This equation has the structure of a Lorentz-force law on the control manifold endowed with the metric $g'_{\mu\nu}$, with $\mathcal{D}_{\text{QGL}}^{\mu\nu(K)} \dot{\lambda}_\nu$ acting as an effective force. The curvature sets the local direction of the

field, while $K(t)$ selects the corresponding Lie-algebra component and plays the role of an effective internal charge. Finally, when $\|F(\boldsymbol{\lambda})\|_{\text{HS}}$ is constant, the conformal factor reduces to a global rescaling, and the loop candidates for QGL optimization coincide with the non-Abelian brachistochrones in the Fubini–Study metric.

Application to the quantum tripod. We illustrate the framework in a paradigmatic non-Abelian system [14, 15, 55]: a tripod configuration with three degenerate ground states coupled to a single excited state. The dynamics is restricted to a two-dimensional dark subspace $\mathcal{D}(t)$ spanned by $|D_j\rangle = e^{i\chi/2}|\tilde{D}_j\rangle$, with $|\tilde{D}_1\rangle = \sin\phi e^{-\frac{i}{2}\varphi}|1\rangle - \cos\phi e^{\frac{i}{2}\varphi}|2\rangle$ and $|\tilde{D}_2\rangle = \cos\theta \cos\phi e^{-\frac{i}{2}\varphi}|1\rangle + \cos\theta \sin\phi e^{\frac{i}{2}\varphi}|2\rangle - \sin\theta|3\rangle$. The control parameters are $\boldsymbol{\lambda}(t) = (\theta, \phi, \varphi)$, while χ generates a trivial gauge transformation. The connection reads $A_\theta = 0_{2\times 2}$, $A_\phi = \cos\theta \sigma_y$, $A_\varphi = \frac{1}{2} \sin(2\phi) \cos\theta \sigma_x - \frac{1}{4} \cos(2\phi) (1 + \cos^2\theta) \sigma_z$, yielding a genuinely non-Abelian structure $[A_\phi, A_\varphi] \neq 0$.

As $\|F\|_{\text{HS}} = \sqrt{3}$ everywhere in the tripod model, we obtain closed candidate loops by solving the quantum brachistochrone in the original Fubini–Study metric $g_{\mu\nu}$. We also compute the corresponding open brachistochrone paths for comparison. We use a shooting method on the parameter set $\{\boldsymbol{\lambda}_0, \dot{\boldsymbol{\lambda}}_0, K_0, T\}$ that enforces both gate fidelity and closure of the parameter trajectory. Figure 1 shows the resulting trajectories for two target gates, $U_1^* = e^{i\frac{\pi}{3}\sigma_y}$ and $U_2^* = e^{i\frac{\pi}{3}\sigma_z}$. For U_1^* , the optimal open trajectory moves predominantly along ϕ , consistent with $A_\phi \propto \sigma_y$, while keeping φ nearly constant to suppress unwanted σ_x and σ_z rotations. For U_2^* , the optimal open trajectory follows the equator $\theta = \pi/2$, where $A_\varphi \propto \sigma_z$. Since $A_\theta = 0$, one may expect optimal trajectories to move at fixed θ , which is approximately realized for open trajectories. Closed holonomies, however, require a finite enclosed area and therefore nonzero curvature flux, forbidding motion along a single coordinate. The associated paths explore at least two directions: (θ, ϕ) for U_1^* and (θ, φ) for U_2^* . The corresponding Fubini–Study lengths are $\mathcal{L}_{1,2}^{(\text{open})} \simeq 0.4$ for open-path implementations, whereas the closed-loop trajectories are substantially longer, $\mathcal{L}_1^{(\text{closed})} = 2.5$ and $\mathcal{L}_2^{(\text{closed})} \simeq 2.7$. This highlights the geometric overhead of closed holonomic implementations relative to open-path non-Abelian gates.

To probe the impact of non-Abelianity on geometric efficiency, we next investigate the tightness of the bounds (4) and (5). We consider the family of target gates $U^*(\alpha) = e^{i\Phi \hat{\mathbf{n}}(\alpha) \cdot \boldsymbol{\sigma}}$, with fixed angle $\Theta(U^*) = \Phi = \pi/4$ and $\hat{\mathbf{n}}(\alpha) = \cos\alpha \hat{\mathbf{y}} + \sin\alpha \hat{\mathbf{z}}$. For each target gate, we first construct a closed contour \mathcal{C} satisfying the holonomy constraint and then determine an associated spanning surface $\Sigma(\mathcal{C})$ minimizing the curvature flux through direct relaxation of the flux functional.

While still more efficient solutions may exist, the

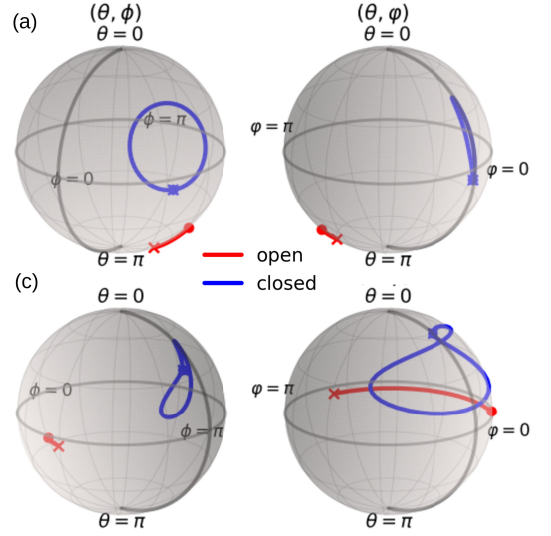


FIG. 1. Non-Abelian brachistochrones: Open (red) and closed (blue) brachistochrones for (a,b) $U_1^* = e^{i\frac{\pi}{3}\sigma_y}$ and (c,d) $U_2^* = e^{i\frac{\pi}{3}\sigma_z}$. (a,c) show the (θ, ϕ) motion on a sphere, while (b,d) represent the (θ, φ) motion. Open brachistochrones follow trajectories close to latitude circles. Target holonomies are reached within $\epsilon = 1 - \mathcal{F} < 10^{-5}$. ($\mathcal{F} = |\langle U^*, U(T) \rangle|^2$)

present scheme provides explicit constructive realizations and corresponding upper bounds on the minimal geometric cost. Our numerical results suggest an optimization landscape with multiple competing branches satisfying the same closure and holonomy constraints. Since $\Theta(U^*) = \Phi$, the efficiency ratio $\eta = \mathcal{A}(\Sigma(\mathcal{C}))/\Phi$ provides a direct measure of the tightness of the bound (5). As shown in Fig. 2, gates whose $SU(2)$ rotation axes are close to the σ_y or σ_z directions ($\alpha \simeq 0, \pi/2$) nearly saturate the Abelian bound. In these regions, the efficiency ratio shows only weak dispersion, indicating that near-optimal solutions are readily found. By contrast, around intermediate orientations, $\hat{\mathbf{n}} \simeq (\hat{\mathbf{y}} + \hat{\mathbf{z}})/\sqrt{2}$, the larger spread signals several competing local minima, and the optimization jumps between distinct branches. To elucidate the conditions for maximal efficiency, we analyze representative near-saturating solutions by reconstructing both the candidate contour and the associated optimized surface, and by monitoring the Lie-algebra direction of the transported curvature over $\Sigma(\mathcal{C})$. Near saturation, the transported curvature is almost collinear across the optimal surface (see inset 1), whereas away from saturation it displays pronounced directional variation (see inset 2). The tighter Abelian bound is therefore approached whenever the curvature becomes effectively Abelian. This indicates that non-Abelianity tends to reduce the QGL-efficiency in the tripod model.

To conclude, we have established quantum geometric limits for non-Abelian holonomies, bounding the magnitude of arbitrary Wilczek–Zee holonomies by curvature-norm costs over spanning surfaces. The associated

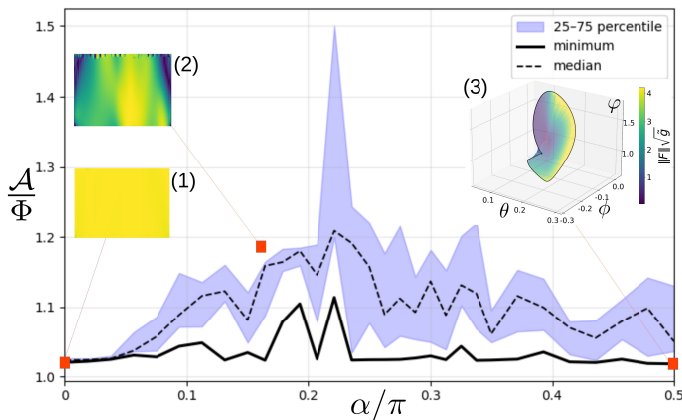


FIG. 2. QGL efficiency $\eta = \mathcal{A}(\Sigma(C))/\Phi$ as a function of the rotation-axis orientation for the target gate $U^*(\alpha) = e^{i\Phi \hat{n}(\alpha) \cdot \sigma}$, with fixed angle $\Phi = \pi/4$ and $\hat{n}(\alpha) = \cos \alpha \hat{y} + \sin \alpha \hat{z}$. For each axis orientation, the optimization was repeated 10 times from different initial seeds. The solid black line shows the lowest-cost solution found for each angle, the dashed line the median over all runs, and the blue shaded region the dispersion across runs. Insets (1,2) display the scalar field $\hat{v}_\sigma(s_1, s_2) \cdot \hat{v}_0$, which measures the local alignment of the transported curvature over the optimal surface. Here $\hat{v}_\sigma(s_1, s_2)$ is the unit vector associated with the Lie-algebra direction of the transported curvature projected onto the local surface element, while \hat{v}_0 denotes its dominant orientation over the optimal surface. A nearly uniform inset indicates that the transported curvature is almost collinear with a single generator, corresponding to near-saturation of the Abelian bound. The 3D inset (3) shows a representative optimal contour and surface for the gate $U_2^* = U^*(\pi/2)$ (angles in units of π), where $\|F\| \equiv \|F\|_{\text{HS}}$ and \sqrt{g} determines the local area element.

optimization defines a coupled contour–surface problem whose boundary dynamics has the form of a non-Abelian Lorentz force. In the tripod model, near-optimal solutions approach QGL saturation by aligning the transported curvature along a single Lie-algebra direction. These results open a route toward quantitative geometric-resource bounds for holonomic and topological quantum computation [9, 59–66] and for condensed-matter phenomena governed by non-Abelian quantum geometry [67–69].

Acknowledgments. We acknowledge support from the Institut Universitaire de France, and from the ANR project QuCoBEC (ANR-22-CE47-0008-02) and from the CAPES-COFECUB (20232475706P) program. F.I. acknowledges support from the Brazilian agencies CNPq (305638/2023-8) and FAPERJ (210.570/2024).

[1] S. Pancharatnam, Generalized theory of interference, and its applications. part i. coherent pencils, *Proceedings of the Indian Academy of Sciences - Section A* **44**, 247

- (1956).
- [2] B. Simon, Holonomy, the quantum adiabatic theorem, and berry’s phase, *Phys. Rev. Lett.* **51**, 2167 (1983).
- [3] M. V. Berry, Quantal phase factors accompanying adiabatic changes, *Proceedings of the Royal Society of London A* **392**, 45 (1984).
- [4] J. Anandan and Y. Aharonov, Geometry of quantum evolution, *Phys. Rev. Lett.* **65**, 1697 (1990).
- [5] M. Nakahara, *Geometry, Topology and Physics*, 2nd ed. (Institute of Physics Publishing, Bristol, 2003).
- [6] A. Bohm, A. Mostafazadeh, H. Koizumi, Q. Niu, and J. Zwanziger, *The Geometric Phase in Quantum Systems* (Springer, Berlin, 2003).
- [7] F. Wilczek and A. Zee, Appearance of gauge structure in simple dynamical systems, *Phys. Rev. Lett.* **52**, 2111 (1984).
- [8] A. Uhlmann, Parallel transport and “quantum holonomy” along density operators, *Reports on Mathematical Physics* **24**, 229 (1986).
- [9] P. Zanardi and M. Rasetti, Holonomic quantum computation, *Physics Letters A* **264**, 94 (1999).
- [10] D. Chruściński and A. Jamiołkowski, *Geometric Phases in Classical and Quantum Mechanics*, Progress in Mathematical Physics, Vol. 36 (Birkhäuser Boston, 2004).
- [11] J. Dai, A. Molochkov, A. J. Niemi, and J. Westerholm, Non-Abelian geometric phases in triangular structures and universal SU(2) control in shape space, [e-print arXiv:2512.24798](https://arxiv.org/abs/2512.24798) (2025).
- [12] L.-M. Duan, J. I. Cirac, and P. Zoller, Geometric manipulation of trapped ions for quantum computation, *Science* **292**, 1695 (2001).
- [13] D. Leibfried, B. DeMarco, V. Meyer, D. Lucas, M. Barrett, J. Britton, W. M. Itano, B. Jelenković, C. Langer, T. Rosenband, and D. J. Wineland, Experimental demonstration of a robust, high-fidelity geometric two ion-qubit phase gate, *Nature* **422**, 412 (2003).
- [14] J. Ruseckas, G. Juzeliūnas, P. Öhberg, and M. Fleischhauer, Non-Abelian gauge potentials for ultracold atoms with degenerate dark states, *Phys. Rev. Lett.* **95**, 010404 (2005).
- [15] F. Leroux, K. Pandey, R. Rehbi, F. Chevy, C. Miniatura, B. Grémaud, and D. Wilkowski, Non-Abelian adiabatic geometric transformations in a cold strontium gas, *Nature Communications* **9**, 3580 (2018).
- [16] Bharath H. M., M. Boguslawski, M. Barrios, L. Xin, and M. S. Chapman, Exploring Non-Abelian geometric phases in spin-1 ultracold atoms, *Phys. Rev. Lett.* **123**, 173202 (2019).
- [17] S. Sugawa, F. Salces-Carcoba, A. R. Perry, Y. Yue, and I. B. Spielman, Second Chern number of a quantum-simulated non-Abelian Yang monopole, *Science* **360**, 1429 (2018).
- [18] M. Hasan, C. S. Madasu, K. D. Rathod, C. C. Kwong, C. Miniatura, F. Chevy, and D. Wilkowski, Wave packet dynamics in synthetic Non-Abelian gauge fields, *Phys. Rev. Lett.* **129**, 130402 (2022).
- [19] C. S. Madasu, C. Mitra, L. Gabardos, K. D. Rathod, T. Zanon-Willette, C. Miniatura, F. Chevy, C. C. Kwong, and D. Wilkowski, Experimental realization of a SU(3) color-orbit coupling in an ultracold gas, *Nature Communications* **16**, 8448 (2025).
- [20] A. A. J. Abdumalikov, J. M. Fink, K. Juliusson, M. Pechal, S. Berger, A. Wallraff, and S. Filipp, Experi-

- mental realization of non-Abelian non-adiabatic geometric gates, *Nature* **496**, 482 (2013).
- [21] Y. Xu, Z. Hua, T. Chen, X. Pan, X. Li, J. Han, W. Cai, Y. Ma, H. Wang, Y. P. Song, Z.-Y. Xue, and L. Sun, Experimental implementation of universal nonadiabatic geometric quantum gates in a superconducting circuit, *Phys. Rev. Lett.* **124**, 230503 (2020).
- [22] C. Zu, W.-B. Wang, L. He, W.-G. Zhang, C.-Y. Dai, F. Wang, and L.-M. Duan, Experimental realization of universal geometric quantum gates with solid-state spins, *Nature* **514**, 72 (2014).
- [23] S. Arroyo-Camejo, A. Lazariev, S. W. Hell, and G. Balasubramanian, Room temperature high-fidelity holonomic single-qubit gate on a solid-state spin, *Nature Communications* **5**, 4870 (2014).
- [24] C. G. Yale, F. J. Heremans, B. B. Zhou, A. Auer, G. Burkard, and D. D. Awschalom, Optical manipulation of the Berry phase in a solid-state spin qubit, *Nature Photonics* **10**, 184 (2016).
- [25] T. Iadecola, T. Schuster, and C. Chamon, Non-Abelian braiding of light, *Physical Review Letters* **117**, 073901 (2016).
- [26] Y.-K. Sun *et al.*, Non-Abelian thouless pumping in photonic waveguides, *Nature Physics* **18**, 1080 (2022).
- [27] M. Parto, C. Leefmans, J. Williams, F. Nori, and A. Marandi, Non-Abelian effects in dissipative photonic topological lattices, *Nature Communications* **14**, 1440 (2023).
- [28] Y. Chen, Y. Fan, G. Larssonneur, J. Xiang, A. He, G. Wang, X.-L. Zhang, G. Ma, Q. Zhou, G. Guo, Y. Su, and X. Guo, High-dimensional non-Abelian holonomy in integrated photonics, *Nature Communications* **16**, 3650 (2025).
- [29] M. Guillot, C. Blanchard, M. Morassi, A. Lemaître, L. Le Gratiet, A. Harouri, I. Sagnes, R.-J. Slager, F. N. Ünal, J. Bloch, and S. Ravets, Measuring non-Abelian quantum geometry and topology in a multi-gap photonic lattice, e-print [arXiv:2511.03894](https://arxiv.org/abs/2511.03894) (2025).
- [30] L. I. Mandelstam and I. E. Tamm, The uncertainty relation between energy and time in nonrelativistic quantum mechanics, *Journal of Physics (USSR)* **9**, 249 (1945).
- [31] J. Anandan and Y. Aharonov, Geometry of quantum evolution, *Phys. Rev. Lett.* **65**, 1697 (1990).
- [32] N. Margolus and L. B. Levitin, The maximum speed of dynamical evolution, *Physica D: Nonlinear Phenomena* **120**, 188 (1998).
- [33] V. Giovannetti, S. Lloyd, and L. Maccone, Quantum limits to dynamical evolution, *Phys. Rev. A* **67**, 052109 (2003).
- [34] M. M. Taddei, B. M. Escher, L. Davidovich, and R. L. de Matos Filho, Quantum speed limit for physical processes, *Physical Review Letters* **110**, 050402 (2013).
- [35] A. del Campo, I. L. Egusquiza, M. B. Plenio, and S. F. Huelga, Quantum speed limits in open system dynamics, *Physical Review Letters* **110**, 050403 (2013).
- [36] S. Deffner and E. Lutz, Quantum speed limit for non-Markovian dynamics, *Physical Review Letters* **111**, 010402 (2013).
- [37] S. Deffner and S. Campbell, Quantum speed limits: from Heisenberg’s uncertainty principle to optimal quantum control, *Journal of Physics A: Mathematical and Theoretical* **50**, 453001 (2017).
- [38] B. Shanahan, A. Chenu, N. Margolus, and A. del Campo, Quantum speed limits across the quantum-to-classical transition, *Physical Review Letters* **120**, 070401 (2018).
- [39] F. Impens, F. M. D’Angelis, F. A. Pinheiro, and D. Guéry-Odelin, Time scaling and quantum speed limit in non-Hermitian hamiltonians, *Phys. Rev. A* **104**, 052620 (2021).
- [40] G. Ness, M. R. Lam, W. Alt, D. Meschede, Y. Sagi, and A. Alberti, Observing crossover between quantum speed limits, *Science Advances* **7**, eabj9119 (2021).
- [41] F. Impens and D. Guéry-Odelin, Approaching the quantum speed limit in quantum gates with geometric control, *Phys. Rev. A* **112**, 042614 (2025).
- [42] H. Nelson and E. Barnes, How fast can a quantum gate be? Exact speed limits from geometry, e-print: [arXiv 2604.23031](https://arxiv.org/abs/2604.23031) (2026).
- [43] O. Sönnernborn, Isoholonomic inequalities and speed limits for cyclic quantum systems, e-print [arXiv:2506.10215](https://arxiv.org/abs/2506.10215) (2025).
- [44] M. B. Halpern, Field-strength and dual variable formulations of gauge theory, *Phys. Rev. D* **19**, 517 (1979).
- [45] D. I. Diakonov and V. Y. Petrov, A formula for the Wilson loop, *Physics Letters B* **224**, 131 (1989).
- [46] K.-I. Kondo, Wilson loop and magnetic monopole through a non-Abelian Stokes theorem, *Phys. Rev. D* **77**, 085029 (2008).
- [47] A. Carlini, A. Hosoya, T. Koike, and Y. Okudaira, Time-optimal quantum evolution, *Phys. Rev. Lett.* **96**, 060503 (2006).
- [48] A. Carlini, A. Hosoya, T. Koike, and Y. Okudaira, Time-optimal unitary operations, *Phys. Rev. A* **75**, 042308 (2007).
- [49] A. Mostafazadeh, Quantum brachistochrone problem and the geometry of the state space in pseudo-Hermitian quantum mechanics, *Phys. Rev. Lett.* **99**, 130502 (2007).
- [50] M. Fleischhauer, A. Imamoglu, and J. P. Marangos, Electromagnetically induced transparency: Optics in coherent media, *Reviews of Modern Physics* **77**, 633 (2005).
- [51] R. G. Unanyan, B. W. Shore, and K. Bergmann, Laser-driven population transfer in four-level atoms: Consequences of non-Abelian geometrical adiabatic phase factors, *Phys. Rev. A* **59**, 2910 (1999).
- [52] D. Møller, L. B. Madsen, and K. Mølmer, Geometric phase gates based on stimulated Raman adiabatic passage in tripod systems, *Phys. Rev. A* **75**, 062302 (2007).
- [53] E. Sjöqvist, D. M. Tong, L. M. Andersson, B. Hessmo, M. Johansson, and K. Singh, Non-adiabatic holonomic quantum computation, *New Journal of Physics* **14**, 103035 (2012).
- [54] D. I. Diakonov and V. Y. Petrov, A formula for the Wilson loop, *Physics Letters B* **224**, 131 (1989).
- [55] (2026), see Supplementary Material at [URL will be inserted by publisher] for additional details on the effective Stokes–Schrödinger construction underlying the QGL framework, the derivation of the Mandelstam–Tamm, Hilbert–Schmidt, and operator-norm QGLs for non-Abelian holonomies, the associated variational and optimal-control equations, the corresponding holonomic brachistochrone equations, and the tripod-model implementation.
- [56] L. Vaidman, Minimum time for the evolution to an orthogonal quantum state, *American Journal of Physics* **60**, 182 (1992).
- [57] Q. Ansel, E. Dionis, F. Arrouas, B. Peaudecerf, S. Guérin, D. Guéry-Odelin, and D. Sugny, Introduction to theoretical and experimental aspects of quantum op-

- timal control, *Journal of Physics B: Atomic, Molecular and Optical Physics* **57**, 133001 (2024).
- [58] L. S. Pontryagin, V. G. Boltyanskii, R. V. Gamkrelidze, and E. F. Mishchenko, *The Mathematical Theory of Optimal Processes* (Wiley, New York, 1962).
- [59] J. Pachos, P. Zanardi, and M. Rasetti, Non-Abelian Berry connections for quantum computation, *Physical Review A* **61**, 010305 (1999).
- [60] A. Y. Kitaev, Fault-tolerant quantum computation by anyons, *Annals of Physics* **303**, 2 (2003).
- [61] C. Nayak, S. H. Simon, A. Stern, M. Freedman, and S. Das Sarma, Non-Abelian anyons and topological quantum computation, *Reviews of Modern Physics* **80**, 1083 (2008).
- [62] D. A. Ivanov, Non-Abelian statistics of half-quantum vortices in p -wave superconductors, *Physical Review Letters* **86**, 268 (2001).
- [63] J. Alicea, Y. Oreg, G. Refael, F. von Oppen, and M. P. A. Fisher, Non-Abelian statistics and topological quantum information processing in 1d wire networks, *Nature Physics* **7**, 412 (2011).
- [64] S. Das Sarma, M. Freedman, and C. Nayak, Majorana zero modes and topological quantum computation, *npj Quantum Information* **1**, 15001 (2015).
- [65] S.-B. Zhang, W. B. Rui, A. Calzona, S.-J. Choi, A. P. Schnyder, and B. Trauzettel, Topological and holonomic quantum computation based on second-order topological superconductors, *Physical Review Research* **2**, 043025 (2020).
- [66] A. Calzona, N. P. Bauer, and B. Trauzettel, Holonomic implementation of CNOT gate on topological Majorana qubits, *SciPost Physics Core* **3**, 014 (2020).
- [67] R. Yu, X.-L. Qi, A. Bernevig, Z. Fang, and X. Dai, Equivalent expression of Z_2 topological invariant for band insulators using the non-Abelian Berry connection, *Physical Review B* **84**, 075119 (2011).
- [68] A. A. Soluyanov and D. Vanderbilt, Computing topological invariants without inversion symmetry, *Physical Review B* **83**, 235401 (2011).
- [69] A. Alexandradinata, X. Dai, and B. A. Bernevig, Wilson-loop characterization of inversion-symmetric topological insulators, *Physical Review B* **89**, 155114 (2014).